

Magnon BEC and various phases of 3D quantum helimagnets under high magnetic field

Hiroaki T. Ueda^{1,2} and Keisuke Totsuka¹

¹ *Yukawa Institute for Theoretical Physics, Kyoto University, Kitashirakawa Oiwake-Cho, Kyoto 606-8502, Japan*

² *Condensed Matter Theory Laboratory, RIKEN, Wako, Saitama 351-0198, Japan*

We study high-field phase diagram and low-energy excitations of three-dimensional quantum helimagnets. Slightly below the saturation field, the emergence of magnetic order may be viewed as Bose-Einstein condensation (BEC) of magnons. The method of dilute Bose gas enables a quantitative analysis of quantum effects in these helimagnets and thereby three phases are found: cone, coplanar fan and a phase-separated one. As an application, we map out the phase diagram of a 3D helimagnet which consists of frustrated J_1 - J_2 chains as a function of frustration and an interchain coupling. Moreover, we also calculate the stability of the 2-magnon bound state to investigate the possibility of the bound-magnon BEC.

PACS numbers: 75.10.Jm, 75.60.-d, 75.30.Kz, 75.45.+j

I. INTRODUCTION

Magnetic frustration introduces several competing states which are energetically close to each other and thereby destabilizes simple ordered states. One way to compromise two or more competing orders is to assume a helical (spiral) spin structure¹. In this paper, we discuss the high-field behavior of a spin-1/2 Heisenberg model with generic interactions:

$$H = \sum_{\langle i,j \rangle} J_{ij} \mathbf{S}_i \cdot \mathbf{S}_j + H \sum_j S_j^z. \quad (1)$$

For the simplest case with one magnetic ion per unit cell, one can easily find the classical ground state by minimizing the Fourier transform of the exchange interactions:

$$\epsilon(\mathbf{q}) = \sum_j \frac{1}{2} J_{ij} \cos(\mathbf{q} \cdot (\mathbf{r}_i - \mathbf{r}_j)), \quad (2)$$

where the summation is taken over all j -sites connected to the i -site by J_{ij} . When $\epsilon(\mathbf{q})$ takes its minima ϵ_{\min} at $\mathbf{q} = \pm\mathbf{Q}$, helical order with the wave number \mathbf{Q} or $-\mathbf{Q}$ appears ($\pm\mathbf{Q}$ are not equivalent to each other).

When the external magnetic field is perpendicular to the spiral plane, the spiral is smoothly deformed into the so-called *cone* state (Fig.1) and this persists until all spins eventually get polarized at the saturation field H_c . When the system has an easy-plane anisotropy and the external field is applied in the spiral plane, on the other hand, the system undergoes a (first-order) metamagnetic transition into a coplanar *fan* phase².

One of the simplest models which exhibit, at least in the classical limit, the helical order is a three-dimensionally coupled Heisenberg chains with nearest-neighbor- (NN) J_1 and next-nearest-neighbor (NNN) J_2 coupling. Because of strong quantum fluctuation in one dimension, the spin-singlet ground state of a single decoupled $S = 1/2$ chain can be quite different^{3,4} from its classical counterpart. However, it is generally expected that interchain couplings may eventually stabilize the classical helical order. In fact, many compounds which contain these 1D-chains as subsystems and display magnetic long-range orders are known (see, for instance, TABLE I. in Ref.5). Despite this naive expectation, even relatively mild quantum fluctuations in three dimensions

may destabilizes the classical ground state in some frustrated systems^{6,7}. Therefore, it would be interesting to explore the possibility that quantum fluctuation replaces the classical cone state with other stable ones e.g. a coplanar fan.

Another interesting feature peculiar to the quantum case is that for a region slightly below the saturation field, we can view the emergence of various kinds of (weak) magnetic order as Bose-Einstein condensation (BEC) of magnons which enables us to use the full machinery of many-body theories⁸. The concept of magnon BEC has been successfully applied to explain various experimental results^{9,10,11}. By using dilute-Bose-gas approach, Batyev and Braginskii¹² discussed magnetic structure near saturation from a general point of view and concluded that this is the case if a certain condition for the bosonic interactions is satisfied.

Recently, helimagnetism attracts renewed interest in the context of multiferroicity¹³ and multiferroic behavior has been reported for various helimagnets. For example, a helimagnetic material LiCuVO_4 may be viewed as coupled quantum $S = 1/2$ J_1 - J_2 chains and, as is expected from the classical theories, exhibits helical spin order¹⁵ and ferroelectricity^{16,17} simultaneously under moderate magnetic field. When the field is very high, on the other hand, this compound shows modulated collinear order¹⁸, which contradicts with the aforementioned classical prediction², and this suggests that quantum fluctuation plays an important role. In these multiferroic materials, external magnetic field provides us with a way of controlling polarization¹⁷ and it is crucial to understand magnetic structures in high magnetic field. However, except for one-dimensional cases, only few reliable results are known for quantum systems so far. Our aim in this paper is to determine the stable spin configurations of 3D spin-1/2 helimagnets in a fully quantum-mechanical manner.

The organization of the present paper is as follows. In Sec. II, we describe how magnon BEC technique is used to determine possible magnetic structures slightly below the saturation field. Our dilute Bose gas approach predicts that in general there are at least three types of quantum phases (*cone*, *fan* and an attraction dominant phase; see FIG.1) in the high-field region. By mapping to an effective Lagrangian, we study the low-energy properties of the cone and the fan phases in Sec. III and show that, on top of the standard Goldstone mode, there is a yet another gapless mode in the fan phase which cor-

responds to translation.

In general, when \mathbf{Q} is commensurate with the underlying lattice, lattice symmetry allows several higher-order interactions which may pin the above gapless translational motion. In Sec. IV, we discuss the effects of commensurability on these phases.

As a concrete example, the phase diagram of a model of coupled $S = 1/2$ J_1 - J_2 chains (J_1 - J_2 - J_3 model) is considered in Sec. V. In this model, we also study the stability of 2-magnon bound state. If the bound-magnon BEC occurs, the transverse magnetic moment vanishes. As a result, we find that, on top of the above three phases, a spin nematic phase appears.

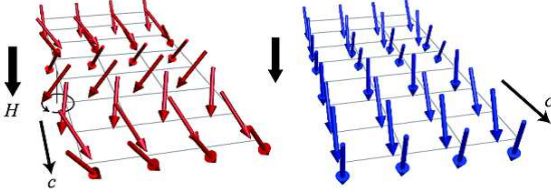


FIG. 1: (Color online) Two spin structures considered here: ‘cone’ (left) and ‘fan’ (right). In the fan structure, the spins are lying in a single plane (*coplanar*). The \mathbf{Q} -vector is pointing along the c -axis.

II. GENERAL FORMALISM

A. Mapping to dilute-Bose gas

To apply the powerful Bose-gas technique, we first rewrite the original spin model in terms of bosons. When the external field H is larger than the saturation field H_c , spins are fully polarized along H (downward, here) and any spin-flip excitations from this reference state can be expressed exactly in terms of hardcore bosons. Specifically, we write the spin operators as:

$$S_l^z = -1/2 + \beta_l^\dagger \beta_l, \quad S_l^+ = \beta_l^\dagger, \quad S_l^- = \beta_l. \quad (3)$$

Then, the original spin Hamiltonian in general may be rewritten in the following way:

$$H = \sum_{\mathbf{q}} (\omega(\mathbf{q}) - \mu) \beta_{\mathbf{q}}^\dagger \beta_{\mathbf{q}} + \frac{1}{2N} \sum_{\mathbf{q}, \mathbf{k}, \mathbf{k}'} V_{\mathbf{q}} \beta_{\mathbf{k}+\mathbf{q}}^\dagger \beta_{\mathbf{k}'-\mathbf{q}}^\dagger \beta_{\mathbf{k}} \beta_{\mathbf{k}'}, \quad (4)$$

$$\begin{aligned} \omega(\mathbf{q}) &= \epsilon(\mathbf{q}) - \epsilon_{\min}, \quad \mu = H_c - H, \\ H_c &= \epsilon(\mathbf{0}) - \epsilon_{\min}, \quad V_{\mathbf{q}} = 2(\epsilon(\mathbf{q}) + U), \end{aligned} \quad (5)$$

where N is the number of lattice sites. In helimagnets, the single-spin flip excitation $\epsilon(\mathbf{q})$ takes its minima ϵ_{\min} at two inequivalent \mathbf{q} -points $\pm\mathbf{Q}$. The external field H controls the chemical potential μ and the on-site interaction $U (\rightarrow \infty)$ has been added to impose the hardcore constraint.

In what follows, we consider a cubic lattice and assume that helical- and ferromagnetic/antiferromagnetic order occur along the c -axis and in the ab plane, respectively (i.e.

$\mathbf{Q} = (0, 0, Q)$ or (π, π, Q)). Also, in order to avoid confusion, we use the indices (a, b, c) for the real-space coordinate and reserve (x, y, z) for the spin directions.

We see that magnon BEC occurs when the external field is smaller than the saturation field: $H < H_c$ ($\mu > 0$). Although the hard-core formulation is valid only for spin-1/2, it can be generalized¹⁹, with a little modification, to arbitrary spin- S .

B. Ginzburg-Landau analysis

The thermal potential per site E/N of the dilute Bose gas is determined by the interaction among the condensed bosons at $\mathbf{q} = \pm\mathbf{Q}$ and the ground-state Boson densities $\rho_{\pm\mathbf{Q}}$ are obtained by minimizing E/N . If we denote the renormalized interactions between the same bosons and that between different ones respectively as Γ_1 and Γ_2 , the energy density E/N is given by

$$\begin{aligned} \frac{E}{N} &= \frac{1}{2} \Gamma_1 (\rho_{\mathbf{Q}}^2 + \rho_{-\mathbf{Q}}^2) + \Gamma_2 \rho_{\mathbf{Q}} \rho_{-\mathbf{Q}} - \mu(\rho_{\mathbf{Q}} + \rho_{-\mathbf{Q}}), \\ &= \frac{1}{4} (\Gamma_1 + \Gamma_2) (\rho_{\mathbf{Q}} + \rho_{-\mathbf{Q}})^2 + \frac{1}{4} (\Gamma_1 - \Gamma_2) (\rho_{\mathbf{Q}} - \rho_{-\mathbf{Q}})^2 \\ &\quad - \mu(\rho_{\mathbf{Q}} + \rho_{-\mathbf{Q}}) \end{aligned} \quad (6)$$

where $\rho_{\mathbf{q}} = |\langle \beta_{\mathbf{q}} \rangle|^2 / N$. First we note that the energy function E/N has discrete \mathbb{Z}_2 -symmetry $\mathbf{Q} \leftrightarrow -\mathbf{Q}$. When the external field H is sufficiently close to the saturation field H_c , we may expect that the condensed boson is dilute and one can safely use the ladder approximation^{8,20} to calculate the interaction vertex (see Fig.2):

$$\begin{aligned} \Gamma_{\mathbf{q}}(\mathbf{k}_1, \mathbf{k}_2) &= V_{\mathbf{q}} - \frac{1}{N} \sum_{\mathbf{q}'} \frac{\Gamma_{\mathbf{q}'}(\mathbf{k}_1, \mathbf{k}_2) V_{\mathbf{q}-\mathbf{q}'}}{\omega(\mathbf{k}_1+\mathbf{q}') + \omega(\mathbf{k}_2-\mathbf{q}') - \omega(\mathbf{k}_1) - \omega(\mathbf{k}_2)}. \end{aligned} \quad (7)$$

From this, one obtains the parameters Γ_1 and Γ_2 as⁷ $\Gamma_1 = \Gamma_0(\mathbf{Q}, \mathbf{Q})$, $\Gamma_2 = \Gamma_0(\mathbf{Q}, -\mathbf{Q}) + \Gamma_{-2\mathbf{Q}}(\mathbf{Q}, -\mathbf{Q})$.

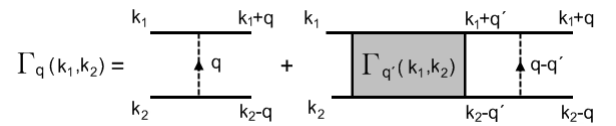


FIG. 2: Ladder approximation to the interaction vertex.

1. Cone phase

Different phases appear according to the values of $\Gamma_{1,2}$. If $\Gamma_2 > \Gamma_1 > 0$, the ground state is given by $\rho_{\mathbf{Q}} = \rho = \mu/\Gamma_1$, $\rho_{-\mathbf{Q}} = 0$ (or vice versa) and $E/N = -\mu^2/(2\Gamma_1)$. Hence, the

spin configuration is determined as:

$$\begin{aligned} \langle \beta_l \rangle &= \sqrt{\rho} \exp\{\pm i(\mathbf{Q} \cdot \mathbf{R}_l + \theta)\}, \langle S_l^z \rangle = -\frac{1}{2} + \rho, \\ \langle S_l^x \rangle &= \sqrt{\rho} \cos(\mathbf{Q} \cdot \mathbf{R}_l + \theta), \langle S_l^y \rangle = \mp \sqrt{\rho} \sin(\mathbf{Q} \cdot \mathbf{R}_l + \theta). \end{aligned} \quad (8)$$

That is, the cone state (the left panel of Fig.1), which exists already in the classical case², is favored for $\Gamma_2 > \Gamma_1$.

It is easy to see that this phase exhibits the multiferroic behavior. According to the so-called spin-current mechanism, a microscopic electric polarization \mathbf{P}_{ij} , which is associated with a pair of sites i and j , is given by^{13,14}

$$\mathbf{P}_{ij} = \eta \mathbf{e}_{ij} \times (\langle \mathbf{S}_i \rangle \times \langle \mathbf{S}_j \rangle), \quad (9)$$

where η is a constant. When the external field \mathbf{H} is parallel to the a (or b)-axis, the \mathbf{Q} -vector is in the spiral plane, which is perpendicular to \mathbf{H} , and the summation of the local polarization \mathbf{P}_{ij} over the lattice yields a finite polarization $\propto \rho Q \sin Q$ parallel to $\mathbf{Q} \times \mathbf{H}$. When \mathbf{H} is along the c -axis, on the other hand, the local polarization sums up to zero and the system shows no ferroelectricity.

2. Fan phase

If $\Gamma_1 > \Gamma_2$ and $\Gamma \equiv \Gamma_1 + \Gamma_2 > 0$, on the other hand, the two modes condense simultaneously and the ground state is determined as: $\rho_{\mathbf{Q}} = \rho_{-\mathbf{Q}} = \rho' = \mu/\Gamma$, $\frac{E}{N} = -\mu^2/\Gamma$

$$\begin{aligned} \langle \beta_l \rangle &= \sqrt{\rho'} \left\{ e^{i(\mathbf{Q} \cdot \mathbf{R}_l + \theta_1)} + e^{i(-\mathbf{Q} \cdot \mathbf{R}_l + \theta_2)} \right\}, \\ \langle S_l^z \rangle &= -\frac{1}{2} + 4\rho' \cos^2(\mathbf{Q} \cdot \mathbf{R}_l + \frac{\theta_1 - \theta_2}{2}), \\ \langle S_l^\pm \rangle &= 2\sqrt{\rho'} \cos(\mathbf{Q} \cdot \mathbf{R}_l + \frac{\theta_1 - \theta_2}{2}) e^{\mp i \frac{\theta_1 + \theta_2}{2}}. \end{aligned} \quad (10)$$

The two parameters θ_1 and θ_2 characterize arbitrary phases of the two condensates $\langle \beta_{\mathbf{Q}} \rangle$ and $\langle \beta_{-\mathbf{Q}} \rangle$, respectively and lead to two different low-energy excitations. Since $\langle S_l^y \rangle / \langle S_l^x \rangle = -\tan \frac{\theta_1 + \theta_2}{2}$, the spins assume a coplanar configuration (*fan*) shown in the right panel of FIG.1.

The ferroelectric property of this phase can be seen again from eq.(9). If one moves from one site to the next along the c -axis, spins change their direction periodically within a basal plane specified by the azimuthal angle $(\theta_1 + \theta_2)/2$ (see FIG.1). Although the vector chirality on each bond ($\langle \mathbf{S}_i \rangle \times \langle \mathbf{S}_{i+e_c} \rangle$) is always pointing a fixed direction perpendicular to the basal plane, it changes the sign within a period; for the first half period, it is positive and for the latter negative. Hence the local polarizations $\mathbf{e}_c \times (\langle \mathbf{S}_i \rangle \times \langle \mathbf{S}_{i+e_c} \rangle)$, when summed up along the c -axis, exactly cancel out and yield zero macroscopic polarization (note that only bonds parallel to the c -axis give non-zero contribution).

Here we would like to stress that the fan state here does not require any kind of easy-plane anisotropy and should be distinguished from its classical counterpart which exists *only* in easy-plane helimagnets². It is interesting to observe that in the second case (*fan*) the ordinary superfluid order ($\langle S^\pm \rangle \neq 0$) and the spin-density wave, where S_l^z modulates with momentum $2\mathbf{Q}$, coexist.

3. Attraction-dominant phase

When $\Gamma_1 < 0$ or $\Gamma_1 + \Gamma_2 < 0$, low-energy bosons around $\mathbf{q} = \pm \mathbf{Q}$ attract each other. If the energy (6) is taken literally, first order transitions may be expected on general grounds. In some cases, this scenario may be the case. However, eq.(6) is based on the assumption that magnon BEC occurs in the single-particle channel and may not work when we expect magnon bound states stabilized by strong attraction. In fact, this conditions for $\Gamma_{1,2}$ implies nothing but instability in the one-magnon condensates. In Sec.V, we calculate the energy of the 2-magnon bound state in the concrete model. As a result, we see that the bound state tends to be favored in attraction-dominant phase.

We summarize the (Γ_1, Γ_2) -phase diagram in FIG. 3. In section V, we shall calculate $\Gamma_{1,2}$ for a specific model and show that all three possible phases appear.

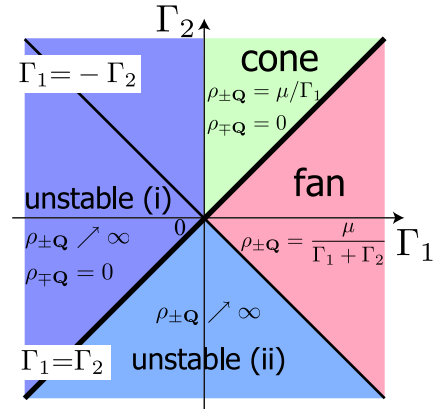


FIG. 3: (Color online) Phase diagram in (Γ_1, Γ_2) -plane. When $\Gamma_1 < 0$ or $\Gamma_1 + \Gamma_2 < 0$, the energy function E/N is, at least within single-particle BEC, unstable (*unstable (i)* and *unstable (ii)*).

III. LOW-ENERGY PROPERTIES

A. Effective Lagrangian

Thus far we have described the general results¹². Now we study the low-energy properties of the two phases more closely. To this end, it is convenient to introduce two independent low-energy modes a and b through

$$\beta_l \sim e^{i\mathbf{Q} \cdot \mathbf{R}_l} a(\mathbf{R}) + e^{-i\mathbf{Q} \cdot \mathbf{R}_l} b(\mathbf{R}). \quad (11)$$

The mass parameters corresponding to these modes are obtained from the low-energy dispersion. Defining $\mathbf{k} \equiv \mathbf{q} - \mathbf{Q}$, we may expand $\epsilon(\mathbf{q}) = \epsilon_{\min} + k_i k_j / (2m_{ij}) + \dots$, ($i, j = a, b, c$) where the summation over repeated indices is implied. The symmetric mass matrix m_{ij} can be diagonalized to give a standard form of the dispersion $k_i k_j / 2m_{ij} = k_i'^2 / (2m_i')$ $\equiv \epsilon_g(\mathbf{k}')$. We assume $m_i > 0$ (for all i) for the stability of the minima at $\mathbf{q} = \pm \mathbf{Q}$. Below we omit the prime over m_j for simplicity. As a result, we write down the following effective

Lagrangian with the renormalized interactions:

$$L_{\text{eff}} = \int d^3\mathbf{x} \left[\frac{i}{2} (a^* \partial_t a - a \partial_t a^*) - \frac{|\partial_j a|^2}{2m_j} + \mu a^* a \right. \\ \left. + \frac{i}{2} (b^* \partial_t b - b \partial_t b^*) - \frac{|\partial_j b|^2}{2m_j} + \mu b^* b \right. \\ \left. - \frac{\Gamma_1}{2} (|a|^4 + |b|^4) - \Gamma_2 |a|^2 |b|^2 \right]. \quad (12)$$

We note that this effective Lagrangian has $U(1) \times U(1)$ symmetry; one comes from the axial (around the external field) symmetry and the other from an *emergent* translational symmetry which does not exist at the level of the lattice. When $\Gamma_1 = \Gamma_2$, this $U(1) \times U(1)$ -symmetry gets enlarged to $U(2)$. On the fully saturated ground state, both a and b bosons have the energy gap $-\mu$.

B. Cone phase

In the case of $\Gamma_2 > \Gamma_1 > 0$, the cone phase appears. Only one of the low-energy bosons (say, a) condenses and we parameterize it as: $a = \sqrt{\rho + \delta\rho} e^{i\theta}$ with $\rho_{\mathbf{Q}} = \rho = \mu/\Gamma_1$. If we integrate out the massive $\delta\rho$ fields in the path integral, we obtain the following effective Lagrangian:

$$L_{\text{cone}} = \int d^3\mathbf{x} \left\{ \left[\frac{(\partial_t \theta)^2}{2\Gamma_1} - \frac{\rho}{2m_j} (\partial_j \theta)^2 \right] \right\} \\ + \frac{i}{2} (b^* \partial_t b - b \partial_t b^*) - \frac{|\partial_j b|^2}{2m_j} + \mu \left(1 - \frac{\Gamma_2}{\Gamma_1}\right) b^* b - \frac{\Gamma_1}{2} |b|^4, \quad (13)$$

From this, we can read off the excitation spectrum of the θ -mode as:

$$\Omega_{\text{cone}}(\mathbf{k}) = \sqrt{2\mu\epsilon_{\mathbf{g}}(\mathbf{k})}, \quad (14)$$

and that of b field acquires a gap $\mu(\frac{\Gamma_2}{\Gamma_1} - 1)$.

C. Fan phase

The low-energy spectrum of the fan phase ($\Gamma_1 > \Gamma_2$, $\Gamma_1 + \Gamma_2 > 0$) exhibits quite a different behavior, since two bosons a and b condense *simultaneously* and the above-mentioned $U(1) \times U(1)$ -symmetry plays a crucial role. To see this more clearly, let us parameterize $a = \sqrt{\rho' + \delta\rho_1} e^{i\theta_1}$, $b = \sqrt{\rho' + \delta\rho_2} e^{i\theta_2}$ and integrate out the massive $\delta\rho_{1,2}$ fields in the path integral. Then L_{eff} reduces to:

$$L_{\text{fan}} = \int d^3\mathbf{x} \left\{ \left[\frac{(\partial_t \theta_u)^2}{2(\Gamma_1 + \Gamma_2)} - \frac{\rho}{2m_j} (\partial_j \theta_u)^2 \right] \right\} \\ + \left\{ \frac{(\partial_t \theta_v)^2}{2(\Gamma_1 - \Gamma_2)} - \frac{\rho}{2m_j} (\partial_j \theta_v)^2 \right\}, \quad (15)$$

where we have introduced $\theta_u \equiv (\theta_1 + \theta_2)/\sqrt{2}$, $\theta_v \equiv (\theta_1 - \theta_2)/\sqrt{2}$. Now the meanings of the two angular variables appearing in eq.(10) are clear; the field θ_u corresponds to the

Goldstone mode associated with the spontaneous breaking of rotational symmetry in the x - y plane, while the other θ_v describes the translational motion of the fan along \mathbf{Q} (*phason* of the spin (S^z) density wave). The excitation spectrum of the θ_u -mode is readily obtained from (15) as

$$\Omega_u(\mathbf{k}) = \sqrt{2(\Gamma_1 + \Gamma_2)\rho'\epsilon_{\mathbf{g}}(\mathbf{k})} = \sqrt{2\mu\epsilon_{\mathbf{g}}(\mathbf{k})} (= \Omega_{\text{cone}}(\mathbf{k})). \quad (16)$$

This gapless excitation does not exist in the fan phase appearing in classical models with easy plane anisotropy². Similarly, the excitation spectrum related to θ_v is given by

$$\Omega_v(\mathbf{k}) = \sqrt{2(\Gamma_1 - \Gamma_2)\rho'\epsilon_{\mathbf{g}}(\mathbf{k})} = \sqrt{2\frac{\Gamma_1 - \Gamma_2}{\Gamma_1 + \Gamma_2}\mu\epsilon_{\mathbf{g}}(\mathbf{k})}. \quad (17)$$

At the transition point $\Gamma_1 = \Gamma_2$ from the cone to the fan, the phonon velocity of the θ_v -mode vanishes indicating an instability in the translational mode.

IV. EFFECTS OF COMMENSURABILITY

In this section, we consider effects of commensurability on the ground state. Since our system is defined on a lattice, any types of interactions which are allowed by the symmetry may be added to the effective Lagrangian (12). Specifically, we require invariance under

- (i) global $U(1)$: $(a, b) \mapsto e^{i\theta}(a, b)$
 - (ii) lattice translation: $a \mapsto a e^{i\mathbf{Q}\cdot\delta}$, $b \mapsto b e^{-i\mathbf{Q}\cdot\delta}$ (18)
- (δ : lattice period).

For generic incommensurate values of \mathbf{Q} , the effective Lagrangian (15) correctly describes the low-energy physics. If Q is rational (i.e. $Q = Q_0 = \pi n/l$: l, n are coprime), on the other hand, the following terms in general appear to break the translational $U(1)$ symmetry explicitly:

$$\frac{1}{2}\Gamma_3 (a^\dagger l b^l + b^\dagger l a^l) \simeq \Gamma_3 \rho^l \cos l(\theta_1 - \theta_2) \\ = \Gamma_3 \rho^l \cos(\sqrt{2} l \theta_v). \quad (19)$$

If we treat the problem in a classical manner, we can imagine an infinite sequence of crystalline phases with superfluid order (spin analogue of supersolids).

However, if we take into account quantum fluctuation, this devil's staircase structure is destroyed and only a finite number of commensurate phases survive²¹. To see this explicitly, we redefine the boson operator as:

$$a(\mathbf{R}) \mapsto e^{-i\delta\mathbf{Q}\cdot\mathbf{R}} a(\mathbf{R}), \quad b(\mathbf{R}) \mapsto e^{+i\delta\mathbf{Q}\cdot\mathbf{R}} b(\mathbf{R}) \\ (\delta\mathbf{Q} \equiv (0, 0, Q - Q_0)). \quad (20)$$

Then, the effective Lagrangian is given as,

$$L_{\text{eff}2} = \int d^3\mathbf{x} \left[\frac{i}{2}(a^* \partial_t a - a \partial_t a^*) - \frac{|(-i\partial_j - \delta Q_j)a|^2}{2m_j} \right. \\ \left. + \mu a^* a + \frac{i}{2}(b^* \partial_t b - b \partial_t b^*) - \frac{|(-i\partial_j + \delta Q_j)b|^2}{2m_j} + \mu b^* b \right. \\ \left. - \frac{\Gamma_1}{2}(|a|^4 + |b|^4) - \Gamma_2 |a|^2 |b|^2 - \frac{\Gamma_3}{2}(a^* b^l + b^* a^l) \right]. \quad (21)$$

From now, we concentrate on the fan phase where both a and b condense. As before, we integrate out the massive $\delta\rho_{1,2}$ fields in the path integral, and ignore the terms which do not matter for low-energy physics when the superfluid density ρ is dilute and $l \geq 3$. For $l = 2$ case, Γ_3 term is the same order as Γ_1 and Γ_2 term in E/N and therefore fan phase appears for²² $\Gamma_1 + |\Gamma_3| > \Gamma_2$. Thus, our approximation may not be justified for $l = 2$ case. Now, $L_{\text{eff}2}$ reads,

$$L'_{\text{eff}2} \approx \int d^3\mathbf{x} \left\{ \frac{(\partial_t \theta_u)^2}{2(\Gamma_1 + \Gamma_2)} - \frac{\rho}{2m_j} (\partial_j \theta_u)^2 \right\} \\ + \left\{ \frac{(\partial_t \theta_v)^2}{2(\Gamma_1 - \Gamma_2)} - \frac{\rho}{2m_j} (\partial_j \theta_v - \sqrt{2}\delta Q_j)^2 - \Gamma_3 \rho^l \cos \sqrt{2}l\theta_v \right\}. \quad (22)$$

Classically, if δQ is small, the Γ_3 -term seems to pin the translation mode θ_v at the expense of the elastic energy. If θ_v is pinned, on the other hand, the gapped zero-point fluctuations around the pinned value yield the (positive) quantum correction to the ground state energy and thereby a soliton lattice with gapless excitations²³ may be favored. From eq.(14) in Ref.21, an incommensurate soliton lattice is stable for any δQ if the following inequality is satisfied:

$$l^2 > \text{Min} \left[16 \left(\frac{\rho}{m_i(\Gamma_1 - \Gamma_2)} \right)^{1/2} \right], \quad (23)$$

where $\text{Min}[\dots]$ means that the minimum value with respect to $i = a, b, c$ should be taken. Therefore, at least in the dilute gas limit, i.e., just below the saturation field, a commensurability locking does not occur for $l \geq 3$. When ρ grows further, eq.(23) may be violated for some small commensurability l and the locking occurs; the pitch Q is locked to its commensurate value Q_0 until δQ exceeds the critical value²¹

$$\delta Q_c^2 = (8/\pi^2) 2m_c |\Gamma_3| \rho^{l-1} \{1 - (l^2/16) \sqrt{m_c(\Gamma_1 - \Gamma_2)/\rho}\}^2. \quad (24)$$

It is interesting to see that the first term, which is obtained by classical calculation, has the same character as a classical fan phase in an easy plane, which has a width proportional to²⁴ $\delta Q^2 \propto |\mathbf{H} - \mathbf{H}_c|^{l-1}$.

Before concluding this section, we would like to give a remark on the validity of our treatment. Above discussions assume the dilute-gas limit, where the scattering length is much smaller than the average interatomic distance $\rho^{-1/3}$. Specifically, our approximation is valid when $\Gamma_i(m_a m_b m_c \rho)^{1/3} \ll 1$ is satisfied for $i = 1$ or 2 .

V. COUPLED J_1 - J_2 MODEL

A. Phases of a single J_1 - J_2 chain

Before presenting our results for a 3D model (J_1 - J_2 - J_3 model), let us briefly review the known results for the $S = 1/2$ J_1 - J_2 chain (the case with $J_3 = 0$) and discuss the connection to the phases found in Sec.II. In the case $J_1 > 0$, near saturation, two dominant phases are found²⁵: (i) ‘chiral phase (VC)’ with finite vector chirality parallel to the magnetic field^{25,26} and (ii) ‘TL2’ phase where the system is described by two Tomonaga-Luttinger (TL) liquids^{25,27}. Obviously, the former turns, after switching on an interchain coupling, into the cone phase. A close inspection of the two gapless TL modes near saturation tells us that the TL2 phase should evolve into the fan phase in three dimensions where we have two Goldstone modes. Yet another dominant phase ‘TL1’, for which a single-component TL gives a good description^{25,26}, is located in a region where we expect a more conventional single-component BEC at $\mathbf{Q} = (0, 0, \pi)$ ($J_3 < 0$) or (π, π, π) ($J_3 > 0$).

The ferromagnetic side $J_1 < 0$ is much more subtle as we expect BECs of n -bound magnon states ($n \geq 2$) to occur. In one-dimension ($J_3 = 0$), on top of the VC phase described above, various phases related to bound n -magnons ($2 \leq n \leq 4$) have been found²⁸; (a) TL phases of 2-magnon bound states ‘nematic’ and ‘SDW₂’, whose dominant correlation occur in respectively superfluid- and SDW channel, (b) 3-magnon TL ‘triatric’ and ‘SDW₃’ (the meanings of them are evident) and (c) ‘quartic’ corresponding to 4-magnon bound states. Our dilute-gas analysis predicts that inside the domes of the attraction-dominant phase (phase (iii) in Fig.4) one-magnon BEC becomes unstable toward various kinds of magnon bindings as has been discussed in Sec.II B 3 and we may expect that the above n -magnon-based phases correspond to the attraction-dominant phase. We also study the stability of the 2-magnon bound state by the traditional approach²⁹ and discuss in later part of this section.

B. 3D phase diagram

Having established the formalism, we now consider a frustrated spin-1/2 model on a simple cubic lattice whose Hamiltonian is given by

$$H = \sum_{\mathbf{r}, i=a,b} \{J_1 \mathbf{S}_{\mathbf{r}} \cdot \mathbf{S}_{\mathbf{r}+\hat{\mathbf{e}}_c} + J_2 \mathbf{S}_{\mathbf{r}} \cdot \mathbf{S}_{\mathbf{r}+2\hat{\mathbf{e}}_c} + J_3 \mathbf{S}_{\mathbf{r}} \cdot \mathbf{S}_{\mathbf{r}+\hat{\mathbf{e}}_i}\}, \quad (25)$$

where we label the three crystal axes by (a, b, c) and the spiral vector \mathbf{Q} is pointing the c -direction. The J_1 - J_2 chains are running in the c -direction and J_3 controls the coupling among adjacent chains.

If we replace the spin-1/2s by hardcore bosons, we obtain the bosonic Hamiltonian (4) with $\epsilon(q)$ given by:

$$\epsilon(q) = J_1 \cos q_c + J_2 \cos 2q_c + J_3 (\cos q_a + \cos q_b). \quad (26)$$

The mass parameters are given by $m_a = m_b = 1/|J_3|$, and $m_c = 1/(4J_2 - J_1^2/4J_2)$. The wave number \mathbf{Q} characterizing

the condensate is given either by $\mathbf{Q} = (0, 0, Q)$ ($J_3 < 0$) or by $\mathbf{Q} = (\pi, \pi, Q)$ ($J_3 > 0$) where $Q = \arccos(-J_1/4J_2)$. We solved eq.(7) to determine the spin structure of our J_1 - J_2 - J_3 model (see Appendix A for the details). As a result, we obtained the phase diagram shown in FIG.4.

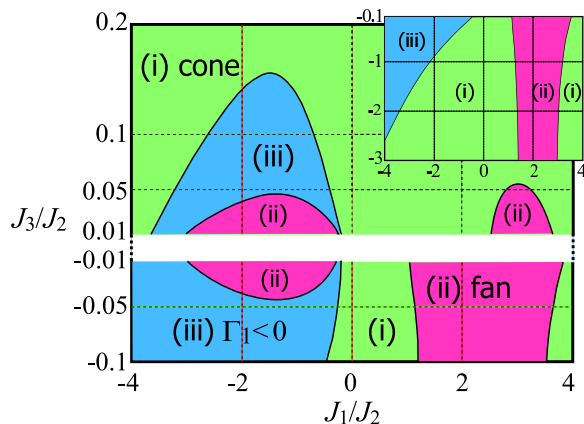


FIG. 4: (Color online) Phase diagram slightly below saturation ($H \lesssim H_c$) mapped out in (J_1, J_3) -plane obtained from the one-magnon-BEC approach ($J_2(> 0)$ is used to set the energy unit). Note that only the region $-4 \leq J_1/J_2 \leq 4$, where cone structure with incommensurate \mathbf{Q} is expected classically, is shown. Two Bose-condensed phases (i) *cone phase* and (ii) *coplanar fan phase* as well as the phase-(iii) which is characterized by $\Gamma_1 < 0$ or $\Gamma_1 + \Gamma_2 < 0$ are shown. The region $|J_3|/J_1 \ll 1$ is omitted (see the text). Inset: The same phase diagram for the large negative interchain coupling ($J_3 < -0.1$).

On top of the ordinary cone phase, strong quantum fluctuation in $S = 1/2$ systems stabilizes two new phases: the coplanar fan ((ii)) and the attraction-dominant phase ((iii)). In the phase-(ii), both gauge symmetry and translation symmetry are broken simultaneously and as a consequence we have two different low-energy (Goldstone) modes $\Omega_u(\mathbf{k})$ (eq.(16)) and $\Omega_v(\mathbf{k})$ (eq.(17)). In the phase-(iii), strong attraction may imply instabilities toward other phases e.g. conventional ferromagnetic one or more exotic multipolar ones²⁸. For $J_3 \rightarrow 0$, low-energy quantum fluctuation destabilizes Γ and our approach cannot be extended to $J_3 = 0$ continuously (Γ becomes $O(J_3^{1/2})$ and $\Gamma_1 \rightarrow \Gamma_2$ at the leading order in J_3).

For the ferromagnetic J_3 , the cone phase (region-(i)) gets wider and wider and the boundary between the cone- and the phase-separated phases approaches the classical phase boundary $J_1/J_2 = -4$ as $|J_3|$ is increased (see the inset of FIG.4). This is easily understood since for very large negative J_3 all spins sitting on each ab -plane behave like a *single large spin* to which classical analysis is applicable and the system may be thought of as a *single chain* running in the c -direction. For the antiferromagnetic coupling ($J_3 > 0$), these novel phases ((ii) and (iii)) appear only in the weak-coupling ($J_3 \ll J_{1,2}$) region.

To see the possible magnon binding more clearly, we plot Γ_i in Fig.5. Although Γ_i behave regularly in the most part of the phase diagram, Γ_1 has poles on the boundary between the fan phase (ii) and the phase-(iii) as is seen in Fig.5. This

implies that near the boundary between the phase-(ii) and (iii) the interaction among bosons becomes singularly large which may lead to new phases. Actually, a pole of a interaction between two particles in general imply an existence of stable bound states. Thus, the one-magnon-BEC approach is not sufficient to see the ground state near this boundary.

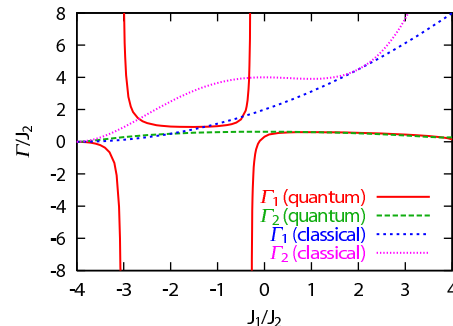


FIG. 5: (Color online) Γ_1 and Γ_2 for $J_3/J_2 = -0.01$ plotted as a function of J_1/J_2 . Also plotted are Γ_i of classical 1D-chain ($J_3 = 0$), where we use the spin-wave expansion around the saturated phase and retain only the leading term of the 4-point interaction in S as in Ref.7. In the classical case, the cone phase is always stable except at $J_1/J_2 = 2$. In the quantum case ($J_3/J_2 = -0.01$), Γ_1 has two poles at the boundaries between the phase (ii) and (iii) in FIG.4.

To highlight this point, we study the instability of the 2-magnon bound state. On the fully saturated ground state $|FM\rangle$, the wave function of the 2-magnon bound state is given by $\sum_{i,j} \psi(i,j) S_i^+ S_j^+ |FM\rangle$, and the energy of this wave function can be exactly obtained by solving the two-body Schrödinger equation²⁹. If the gap of the bound state closes earlier than that of the one magnon, the bound-magnon BEC will occur, and the nematic order emerges in the transverse direction. We show the region of the stable bound state in Fig.6. As a result, the nematic phase completely masks the fan phase which would have appeared on the ferromagnetic side $J_1 < 0$. At a rough estimate, for $-2.7 \lesssim J_1/J_2$, the lowest-mode of the bound state is commensurate and for $J_1/J_2 \lesssim -2.7$ the one is incommensurate in the same way as in the 1D J_1 - J_2 chain^{30,31}.

Detailed results on the bound magnons be reported elsewhere³².

VI. SUMMARY

By using the dilute-Bose-gas technique, we studied the high-field magnetic structures and low-energy excitations of three-dimensional quantum ($S = 1/2$) helimagnet. The method used is asymptotically exact when magnetization is close to saturation (we gave a criterion of ‘proximity’ in the end of section IV) and enables us to obtain reliable results for *three-dimensional* frustrated systems.

In the vicinity of saturation, the original (quantum) spin system may be described in terms of interacting spin-flip magnons. We discussed various phases emerging from the

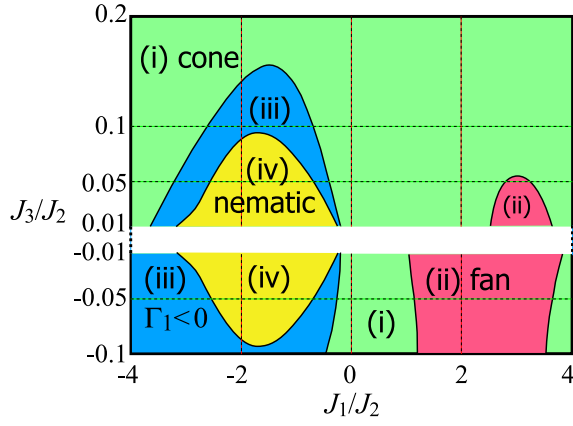


FIG. 6: (Color online) The same phase diagram as in Fig.4 when the 2-magnon bound state is taken into account. The phase (iv) is characterized by the condensation of the 2-magnon bound state and leads to the nematic order in the transverse direction.

BEC of those magnons in Sec. II. Although only the cone phase is expected in the classical helimagnets², quantum fluctuation can stabilize the fan or attraction dominant phases as well according to the renormalized interactions (Γ_1, Γ_2).

Then, the low-energy excitations of the cone and the fan phases were studied in Sec. III. The hallmark of quantum helimagnets is that one has two low-energy modes at $\mathbf{k} = \pm\mathbf{Q}$ and the low-energy physics is described by the effective Lagrangian with $U(1) \times U(1)$ symmetry; one comes from the axial (around the external field) symmetry and the other from an *emergent* translational symmetry. In the cone phase, only one of the two bosons condenses and there is one gapless Goldstone mode (the two $U(1)$ s are no longer independent). Meanwhile, the fan phase breaks both symmetries and has two types of gapless Goldstone modes.

In Sec. IV, we considered effects of commensurability on the helical modulation vector Q . If Q is rational (i.e. $Q = Q_0 = \pi n/l$: l, n are coprime), the interaction term which explicitly breaks the translational $U(1)$ symmetry appears in the effective Lagrangian and favors the gapped commensurate phase. On the other hand, as is well-known in the theory of CDW, the gapped zero-point fluctuations yield the (positive) quantum correction to the ground state energy and thereby a soliton lattice with gapless excitations²³ may be favored. By examining the effective Lagrangian, which is valid for $l \geq 3$ case, we found that slightly below the saturation field quantum fluctuation destroys the commensurate order.

We studied a concrete three-dimensional model which consists of frustrated $S = 1/2$ J_1 - J_2 (nearest-neighbor J_1 and next-nearest-neighbor $J_2 (> 0)$) chains coupled by an interchain interaction J_3 in Sec. V and mapped out its (high-field) phase diagram in Figs.4 and 6. An analysis assuming the single-magnon BEC predicts the existence of a fairly large region where single-magnon BECs may be unstable (phase-(iii)) as well as the cone and the fan shown in Fig.1. To get an insight into the nature of this ‘phase’, we consider the possibility of a BEC of *two-magnon* bound states, which leads to

the nematic order in the transverse direction. In fact, in a large portion of the phase-(iii) (a region marked as (iv) in Fig.6), we have a stable two-magnon bound states which condense first when the external field is decreased. In the 1D J_1 - J_2 model (i.e. $J_3 = 0$), it is known that one has multiple-magnon bound states up to four-body²⁸ and some parts of the new phase (*nematic* (iv) in Fig.6) could be replaced by the condensed phases of these bound states. The detail of the analysis along this line will be reported in a separate publication.

Finally, we comment on the relevance of our study to real systems. Interests in multiferroicity sparked an intensive study of various helimagnetic materials, among which one can find many examples of coupled J_1 - J_2 chains. For example, LiCuVO_4 is characterized by edge-sharing CuO_2 plaquettes and may be modeled by the $S = 1/2$ J_1 - J_2 chain with negative J_1 . Neutron diffraction and *ab initio* calculations suggested¹⁵, as well as J_1 and J_2 , various kinds of interchain interactions J_3, \dots, J_6 . Although the stacking of J_1 - J_2 chains is different from what is assumed here, our method can be readily generalized to include more realistic cases and we hope our approach will shed some light on magnetism of these quantum helimagnets.

Acknowledgments

We thank S. Furukawa, A. Furusaki, T. Hikihara, T. Momoi, T. Nishino, M. Sato, and N. Shannon for discussions. One of us (K.T.) was supported by Grant-in-Aid for Scientific Research (C) 20540375 and that on Priority Areas ‘‘Novel States of Matter Induced by Frustration’’ (No.19052003) from MEXT, Japan. This work was also supported by the Grant-in-Aid for the Global COE Program ‘‘The Next Generation of Physics, Spun from Universality and Emergence’’ from MEXT of Japan.

APPENDIX A: HOW TO TREAT THE LADDER DIAGRAM

For convenience, we briefly summarize the method of calculating Γ . To obtain $\Gamma_1 = \Gamma_{\mathbf{q}=0}(\mathbf{k}_1 = \mathbf{Q}, \mathbf{k}_2 = \mathbf{Q})$ and $\Gamma_2 = \Gamma_0(\mathbf{Q}, -\mathbf{Q}) + \Gamma_{-2\mathbf{Q}}(\mathbf{Q}, -\mathbf{Q})$, we solve the following integral equation in the case of $\mathbf{k}_{1,2} = \pm\mathbf{Q}$ ($\omega(\mathbf{k}_{1,2}) = 0$):

$$\Gamma_{\mathbf{q}}(\mathbf{k}_1, \mathbf{k}_2) = V_{\mathbf{q}} - \frac{1}{N} \sum_{\mathbf{q}'} \frac{\Gamma_{\mathbf{q}'}(\mathbf{k}_1, \mathbf{k}_2) V_{\mathbf{q}-\mathbf{q}'}}{\omega(\mathbf{k}_1 + \mathbf{q}') + \omega(\mathbf{k}_2 - \mathbf{q}')}, \quad (\text{A1})$$

where $V_{\mathbf{q}} = 2(\epsilon(\mathbf{q}) + U)$. In what follows, we do not write the argument $\mathbf{k}_{1,2}$ of Γ explicitly, and denote $\frac{1}{N} \sum_{\mathbf{q}}$ as $\langle \cdot \rangle$. Since $\langle \epsilon \rangle = 0$, we sum up the both side of (A1) with respect to \mathbf{q} and obtain,

$$\langle \Gamma \rangle = 2U \left(1 - \frac{1}{N} \sum_{\mathbf{q}'} \frac{\Gamma_{\mathbf{q}'}}{\omega(\mathbf{k}_1 + \mathbf{q}') + \omega(\mathbf{k}_2 - \mathbf{q}')} \right), \quad (\text{A2})$$

Using this equation, (A1) is simplified to,

$$\Gamma_{\mathbf{q}} = 2\epsilon(\mathbf{q}) + \langle \Gamma \rangle - \frac{1}{N} \sum_{\mathbf{q}'} \frac{2\epsilon(\mathbf{q} - \mathbf{q}')}{\omega(\mathbf{k}_1 + \mathbf{q}') + \omega(\mathbf{k}_2 - \mathbf{q}')} \Gamma_{\mathbf{q}-\mathbf{q}'} . \quad (\text{A3})$$

Additionally, if we assume the limit $U \rightarrow \infty$, eq.(A2) reads:

$$1 - \frac{1}{N} \sum_{\mathbf{q}} \frac{\Gamma_{\mathbf{q}'}}{\omega(\mathbf{k}_1 + \mathbf{q}') + \omega(\mathbf{k}_2 - \mathbf{q}')} = 0 . \quad (\text{A4})$$

Now, the problem is reduced to solve (A3) and (A4) simultaneously, which are free from the infinite term U . Next, we expand $\Gamma_{\mathbf{q}}$ in lattice harmonics. Since

$$\begin{aligned} \epsilon(\mathbf{q} - \mathbf{q}') = & J_1(\cos q_c \cos q'_c + \sin q_c \sin q'_c) \\ & + J_2(\cos 2q_c \cos 2q'_c + \sin 2q_c \sin 2q'_c) \\ & + J_3(\cos q_a \cos q'_a + \sin q_a \sin q'_a \\ & + \cos q_b \cos q'_b + \sin q_b \sin q'_b) , \end{aligned} \quad (\text{A5})$$

$$\begin{aligned} & \left(J_1 A_1 + \frac{1}{N} \sum_{\mathbf{q}'} \frac{2J_1 \cos q'_c}{\omega(\mathbf{k}_1 + \mathbf{q}') + \omega(\mathbf{k}_2 - \mathbf{q}')} \Gamma_{\mathbf{q}'} - 2J_1 \right) \cos q_c + \left(J_1 A_2 + \frac{1}{N} \sum_{\mathbf{q}'} \frac{2J_1 \sin q'_c}{\omega(\mathbf{k}_1 + \mathbf{q}') + \omega(\mathbf{k}_2 - \mathbf{q}')} \Gamma_{\mathbf{q}'} \right) \sin q_c \\ & + \left(J_2 A_3 + \frac{1}{N} \sum_{\mathbf{q}'} \frac{2J_2 \cos 2q'_c}{\omega(\mathbf{k}_1 + \mathbf{q}') + \omega(\mathbf{k}_2 - \mathbf{q}')} \Gamma_{\mathbf{q}'} - 2J_2 \right) \cos 2q_c + \left(J_2 A_4 + \frac{1}{N} \sum_{\mathbf{q}'} \frac{2J_2 \sin 2q'_c}{\omega(\mathbf{k}_1 + \mathbf{q}') + \omega(\mathbf{k}_2 - \mathbf{q}')} \Gamma_{\mathbf{q}'} \right) \sin 2q_c \\ & + \left(J_3 A_5 + \frac{1}{N} \sum_{\mathbf{q}'} \frac{J_3(\cos q'_a + \cos q'_b)}{\omega(\mathbf{k}_1 + \mathbf{q}') + \omega(\mathbf{k}_2 - \mathbf{q}')} \Gamma_{\mathbf{q}'} - 2J_3 \right) (\cos q_a + \cos q_b) = 0 , \end{aligned} \quad (\text{A7})$$

where we use the relation

$$\frac{1}{N} \sum_{\mathbf{q}'} \frac{\sin q'_{x,y}}{\omega(\mathbf{k}_1 + \mathbf{q}') + \omega(\mathbf{k}_2 - \mathbf{q}')} \Gamma_{\mathbf{q}'} = 0 . \quad (\text{A8})$$

To satisfy the eq.(A7) for arbitrary \mathbf{q} , the coefficients of trigonometric function of \mathbf{q} must be 0. For convenience, we define

$$\tau_{ij}(k_1, k_2) = \frac{1}{N} \sum_{\mathbf{q}'} \frac{T_i(q') T_j(q')}{\omega(k_1 + q') + \omega(k_2 - q')} , \quad (\text{A9})$$

$$\begin{pmatrix} \tau_{11} & J_1 \tau_{12} & J_1 \tau_{13} & J_2 \tau_{14} & J_2 \tau_{15} & J_3 \tau_{16} \\ 2\tau_{21} & 1 + 2J_1 \tau_{22} & 2J_1 \tau_{23} & 2J_2 \tau_{24} & 2J_2 \tau_{25} & 2J_3 \tau_{26} \\ 2\tau_{31} & 2J_1 \tau_{32} & 1 + 2J_1 \tau_{33} & 2J_2 \tau_{34} & 2J_2 \tau_{35} & 2J_3 \tau_{36} \\ 2\tau_{41} & 2J_1 \tau_{42} & 2J_1 \tau_{43} & 1 + 2J_2 \tau_{44} & 2J_2 \tau_{45} & 2J_3 \tau_{46} \\ 2\tau_{51} & 2J_1 \tau_{52} & 2J_1 \tau_{53} & 2J_2 \tau_{54} & 1 + 2J_2 \tau_{55} & 2J_3 \tau_{56} \\ \tau_{61} & J_1 \tau_{62} & J_1 \tau_{63} & J_2 \tau_{64} & J_2 \tau_{65} & 1 + J_1 \tau_{66} \end{pmatrix} \begin{pmatrix} \langle \Gamma \rangle \\ A_1 \\ A_2 \\ A_3 \\ A_4 \\ A_5 \end{pmatrix} = \begin{pmatrix} 1 \\ 2 \\ 0 \\ 2 \\ 0 \\ 2 \end{pmatrix} \quad (\text{A11})$$

This equation can be solved by calculating τ_{ij} numerically. If we evaluate at $(\mathbf{k}_1, \mathbf{k}_2) = (\mathbf{Q}, \mathbf{Q})$, $A_2 = A_4 = 0$ due to the

we introduce

$$\begin{aligned} \Gamma_{\mathbf{q}} = & \langle \Gamma \rangle + J_1 A_1 \cos q_c + J_1 A_2 \sin q_c + J_2 A_3 \cos 2q_c \\ & + J_2 A_4 \sin 2q_c + J_3 A_5 (\cos q_a + \cos q_b) . \end{aligned} \quad (\text{A6})$$

We note that $\langle \Gamma \rangle$ and A_i are independent of \mathbf{q} , but depend on $(\mathbf{k}_1, \mathbf{k}_2)$ implicitly. If we substitute this, eq.(A3) reduces to,

where

$$\mathbf{T}(q) = (1, \cos q_c, \sin q_c, \cos 2q_c, \sin 2q_c, \cos q_a + \cos q_b) . \quad (\text{A10})$$

Then, (A4) and (A7) are put together into

symmetry and we obtain,

$$\Gamma_1 = \langle \Gamma \rangle + J_1 A_1 + J_2 A_3 + 2J_3 A_5 . \quad (\text{A12})$$

If we evaluate at $(\mathbf{k}_1, \mathbf{k}_2) = (\mathbf{Q}, -\mathbf{Q})$, we obtain

$$\begin{aligned} \Gamma_2 = & [\langle \Gamma \rangle + J_1 A_1 + J_2 A_3 + 2J_3 A_5] \\ & + [\langle \Gamma \rangle + J_1 A_1 \cos(-2Q) + J_1 A_2 \sin(-2Q) \\ & + J_2 A_3 \cos(-4Q) + J_2 A_4 \sin(-4Q) + 2J_3 A_5] , \end{aligned} \quad (\text{A13})$$

Although above we review the straightforward method, we can calculate Γ_2 more simply if we introduce,

$$\begin{aligned} \Gamma_{\mathbf{q}-\mathbf{Q}}(\mathbf{Q}, -\mathbf{Q}) + \Gamma_{-\mathbf{q}-\mathbf{Q}}(\mathbf{Q}, -\mathbf{Q}) \\ = 2\langle \Gamma \rangle + J_1 A'_1 \cos q_c + J_2 A'_2 \cos 2q_c \\ + J_3 A'_3 (\cos q_a + \cos q_b) . \end{aligned} \quad (\text{A14})$$

The following procedure is the same as in the former case, and Γ_2 is given by,

$$\Gamma_2 = 2\langle \Gamma \rangle + J_1 A'_1 \cos Q + J_2 A'_2 \cos 2Q - 2|J_3|A'_3 . \quad (\text{A15})$$

-
- ¹ A. Yoshimori, J.Phys.Soc.Jpn. **14**, 807 (1959).
² T. Nagamiya, K. Nagata and Y. Kitano, Prog.Theor.Phys. **27**, 1253 (1962); T. Nagamiya, Solid State Physics, Vol. **20**, 305, Academic Press (1967).
³ F.D.M. Haldane, Phys.Rev.B **25**, 4925 (1982); T. Tonegawa and I. Harada, J. Phys. Soc. Jpn. **56**, 2153 (1987); K. Okamoto and K. Nomura, Phys.Lett.A **169**, 433 (1992).
⁴ R. Bursill, G.A. Gehring, D.J.J. Farnell, J.B. Parkinson, T. Xiang and C. Zeng, J.Phys. condensed matter, **7**, 8605 (1995); A. Kolezhuk, R. Roth and U. Schollwöck, Phys.Rev.Lett. **77**, 5142 (1996).
⁵ M. Hase, H. Kuroe, K. Ozawa, O. Suzuki, H. Kitazawa, G. Kido, and T. Sekine, Phys.Rev. B **70**, 104426 (2004).
⁶ T. Nikuni and H. Shiba, J.Phys.Soc.Jpn. **62**, 3268 (1993).
⁷ T. Nikuni and H. Shiba, J.Phys.Soc.Jpn. **64**, 3471 (1995).
⁸ H. Shi and A. Griffin, Phys.Rep. **304**, 1 (1998).
⁹ T. Giamarchi, C. Rüegg and O. Tchernyshyov, Nature Physics **4**, 198 (2008).
¹⁰ T. Nikuni, M. Oshikawa, A. Oosawa and H. Tanaka, Phys.Rev.Lett. **84**, 5868 (2000).
¹¹ T. Radu, H. Wilhelm, V. Yushankhai, D. Kovrizhin, R. Coldea, Z. Tylczynski, T. Lühmann, and F. Steglich Phys.Rev.Lett. **95**, 127202 (2005).
¹² E.G. Batyev and L.S. Braginskii, Zh.Eksp.Teor.Fiz. **87**, 1361 (1984) [Sov.Phys.JETP **60**, 781 (1984)].
¹³ See e.g. S-W. Cheong and M. Mostovoy, Nature materials, **6**, 13 (2007); N. Nagaosa, J.Phys. condensed matter, **20**, 434207 (2008) for reviews.
¹⁴ H. Katsura, N. Nagaosa, and A.V. Balatsky, Phys.Rev.Lett. **95**, 057205 (2005).
¹⁵ B.J. Gibson, R.K. Kremer, A.V. Prokofiev, W. Assmus, G.J. McIntyre, Physica B**350**, e253 (2004); M. Enderle, C. Mukherjee, B. Fåk, R.K. Kremer, J.M. Broto, H. Rosner, S.L. Drechsler, J. Richter, J. Malek, A. Prokofiev, W. Assmus, S. Pujos, J.-L. Raggazzoni, H. Rakoto, M. Rheinstädter and H.M. Rønnow, Europhys.Lett. **70**, 237 (2005).
¹⁶ Y. Naito, K. Sato, Y. Yasui, Y. Kobayashi, Y. Kobayashi, and M. Sato, J.Phys.Soc.Jpn., **76**, 023708 (2007).
¹⁷ F. Schrettle, S. Krohns, P. Lunkenheimer, J. Hemberger, N. Büttgen, H.A. Krug von Nidda, A. V. Prokofiev, and A. Loidl, Phys.Rev. B **77**, 144101 (2008).
¹⁸ N. Büttgen, H.A. Krug von Nidda, L.E. Svistov, L.A. Prozorova, A. Prokofiev and W. Aßmus, Phys.Rev. B **76**, 014440 (2007); M.G. Banks, F.Heidrich-Meisner, A. Honecker, H. Rakoto, J.M. Broto and R.K. Kremer, J. Phys.:Condens. Matter **19**, 145227 (2007).
¹⁹ E.G. Batyev, Zh.Eksp.Teor.Fiz. **89**, 308 (1985) [Sov.Phys.JETP **62**, 173 (1985)].
²⁰ We will discuss the validity of our dilute-Bose-gas approach in the end of section IV.
²¹ P. Bak, and H. Fukuyama, Phys.Rev. B **21**, 3287 (1980).
²² G. Jackeli and M.E. Zhitomirsky, Phys.Rev.Lett. **93**, 017201 (2004).
²³ W.L. McMillan, Phys.Rev. B **16**, 4655 (1977); V.L. Pokrovsky, Solid State Commun. **26**, 77 (1978).
²⁴ J.L. Cadore and C.S.O. Yokoi, Phys.Rev. B **56**, 11635 (1997).
²⁵ K. Okunishi, J.Phys.Soc.Jpn., **77**, 114004 (2008); T. Hikihara, T. Momoi, A. Furusaki and H.Kawamura, unpublished.
²⁶ A. Kolezhuk and T. Vekua, Phys.Rev. B **72**, 094424 (2005); I.P. McCulloch, R. Kube, M. Kurz, A. Kleine, U. Schollwöck, and A.K. Kolezhuk, Phys.Rev. B **77**, 094404 (2008).
²⁷ K. Okunishi, Y. Hieida, and Y. Akutsu, Phys.Rev. B **60**, R6953 (1999); K. Okunishi and T. Tonegawa, J.Phys.Soc.Jpn **72**, 479 (2003).
²⁸ T. Hikihara, L. Kecke, T. Momoi, and A. Furusaki, Phys.Rev. B **78**, 144404 (2008); J. Sudan, A. Luscher, A. Laeuchli, arXiv cond-mat 0807.1923.
²⁹ D.C. Mattis, *The Theory of Magnetism Made Simple* (World Scientific, 2006).
³⁰ A.V. Chubukov, Phys.Rev. B **44**, 4693 (1991).
³¹ For more detail of magnon bound states, see, for example, D.V. Dmitriev and V.Ya. Krivnov, Phys.Rev. B **79**, 054421 (2009) and references cited therein.
³² H.T. Ueda, K. Totsuka and T. Momoi, unpublished.